

Characteristics of Extra Narrow Gap Weld of HSLA Steel Welded by Single-Seam per Layer Pulse Current GMA Weld Deposition

B.P. Agrawal and P.K. Ghosh

(Submitted June 23, 2015; in revised form December 23, 2016; published online February 7, 2017)

Butt weld joints are produced using pulse current gas metal arc welding process by employing the technique of centrally laid multi-pass single-seam per layer weld deposition in extra narrow groove of thick HSLA steel plates. The weld joints are prepared by using different combination of pulse parameters. The selection of parameter of pulse current gas metal arc welding is done considering a summarized influence of simultaneously interacting pulse parameters defined by a dimensionless hypothetical factor ϕ . The effect of diverse pulse parameters on the characteristics of weld has been studied. Weld joint is also prepared by using commonly used multi-pass multi-seam per layer weld deposition in conventional groove. The extra narrow gap weld joints have been found much superior to the weld joint prepared by multi-pass multi-seam per layer deposition in conventional groove with respect to its metallurgical characteristics and mechanical properties.

Keywords characterization, extra narrow gap weld, parameters, pulse current GMAW, single-seam per layer, thick HSLA steel

1. Introduction

High-strength low-alloy (HSLA) steel is widely used by industries in construction of large variety of advanced structures as oil and gas pipelines, heavy-duty road transport vehicles, industrial equipment, storage tanks, mine and railroad cars, bridges and offshore structures, etc. (Ref 1). In order to meet the requirements in various applications, a number of different types of HSLA steel with varying chemical composition of diverse thickness are available. Because of involvement of welding in fabrication of most of the structures, the weldability of these steels gets paramount importance. Although the HSLA steels are good weldable primarily due to their relatively low carbon and alloying content, it is preferred to have low severity of thermal effect during welding of these steels especially to avoid extensive loss of their unique metallurgical characteristics and mechanical properties in heat-affected zone (HAZ).

HSLA steels with thick sections are commonly welded by using arc welding process (Ref 2) such as submerged arc welding (SAW), shielded metal arc welding (SMAW), gas tungsten arc welding (GTAW), and gas metal arc welding

(GMAW). All these welding processes severely influence the weld thermal behavior in different manner largely depending upon their process parameter, welding procedure affecting the amount and quality of weld deposition and geometry of weld bead. The arc welding of thick sections using conventional weld groove becomes relatively more critical primarily because of large amount of multi-pass metal deposition resulting into a cumulative effect of severity of weld thermal cycle (Ref 3). This can be considerably minimized by reducing the amount of weld deposition and its heat content in a joint, obtained through use of narrow gap welding technique (Ref 4, 5). The narrow gap welding is successfully employed in SAW process but, in spite of that, inherently it requires relatively higher heat inputs, which often adversely affects the metallurgical characteristics and mechanical properties of weld joint. The preparation of narrow groove weld joint by SMAW and GTAW processes usually requires welding at a low angle of attack to groove wall by a skilled welder, which makes automation of the process highly critical and complicated. The SAW and SMAW has further limitation of the possibility of entrapment of slag resulting in poor mechanical properties, whereas in case of using GTAW process, the welding speed becomes appreciably low. These limitations of SMAW and GTAW processes can be well addressed by the merits of GMAW process using spray mode of metal transfer. But, depending upon material, size of filler wire, and shielding environment, the spray transfer mode in GMAW may be obtained at fairly high welding current, which can considerably increase heat input to the weld. This enhancement of heat input consequently affects size of weld pool and temperature along with grain coarsening in HAZ affecting negatively its properties. However, the effective heat input to the weld can be considerably minimized with the use of comparatively low heating pulse current gas metal arc welding (P-GMAW) through a control of heat distribution to the weld under pulse current (Ref 6).

The reduction in severity of weld thermal behavior of narrow gap weld can be largely governed by narrowness of the

The newly developed multi-pass single-seam per layer extra narrow gap (MPSSPL-ENG) P-GMAW welding process as discussed in this paper is registered under Indian patent Application No. 1023/Del/2010 Dated 29.04.2010.

B.P. Agrawal, School of Mechanical Engineering, Galgotias University, Greater Noida, G. B. Nagar, Uttar Pradesh 201308, India; and **P.K. Ghosh**, Indian Institute of Technology Roorkee, Roorkee 247667, India. Contact e-mails: banshiprasad@gmail.com, prakgfm@gmail.com.

groove width due to its ability to significantly reduce amount of weld metal deposition producing a sound weld joint of a given thickness. Thus, using an extra narrow groove defined by a significantly lower groove width than that of conventional narrow groove GMA welding may provide further advantage to this aspect. However, the issue of narrowing down groove width in case of GMAW is primarily dictated by the suitability of appropriate torch manipulation up to a desired location at the bottom of the groove maintaining a required angle of attack to the groove wall during welding of a thick section. In this context, exploring the use of GMAW with vertically placed narrow torch nozzle having no angle of attack to the groove wall allowing centrally laid weld deposition in the groove, may provide a further mileage to this issue. But, a major hurdle on this aspect may arise out of proneness of such technique to suffer from lack of groove wall fusion, largely due to availability of inadequate heat on the groove surface in contact with the super-heated weld metal. This is primarily arising out of inappropriate thermal distribution in weld pool. This matter has been successfully addressed with the help of a model analysis based on thermal and geometrical aspects of P-GMA weld pool as reported earlier (Ref 4). The model considers the heat input to the molten weld pool and its transmission to the groove wall from two sources, one being transfer of heat by super-heated filler metal droplets deposited in the weld pool and other one due to transfer of arc heat as double ellipsoidal heat source. With the help of the model analysis, a successful application of P-GMAW at appropriate pulse parameter to produce sound extra narrow groove weld having no lack of groove wall fusion has also been reported earlier (Ref 4).

To establish the utility of newly proposed multi-pass single-seam per layer extra narrow gap (MPSSPL-ENG) P-GMA welding process over the commonly used multi-pass multi-seam per layer conventional groove (MPMSPL-CG) P-GMA welding process, it requires a thorough study on improvement in properties of the weld joint as a function of welding parameters. The optimization of P-GMAW parameters is a quite complex and critical task due to involvement of relatively large number of simultaneously interactive pulse parameters characterizing the implication of pulse current in P-GMAW process. However, a solution to critical control of pulse parameters, such as mean current (I_m), pulse current (I_p), base current (I_b), pulse time (t_p), base time (t_b) and pulse frequency (f) at a given arc voltage (V), for a desired operation of P-GMAW process has been addressed by considering a summarized influence of pulse parameters, the effectiveness of which is amply justified in earlier works (Ref 5-9). It is defined by a dimensionless hypothetical factor $\phi = \left(\frac{I_b}{I_p}\right) \times ft_b$ derived on the basis of energy balance concept (Ref 10, 11) where, $t_b = \left(\frac{1}{f}\right) - t_p$.

In consideration of the above an effort has been made in this work to study the microstructure and mechanical properties of weld joint prepared by using MPSSPL-ENG welding of thick HSLA steel plates. The observations have been compared with properties of the MPMSPL-CG weld of the same material in order to identify the superiority of the newly developed MPSSPL-ENG welding procedure. The use of such a MPSSPL-ENG welding procedure may be beneficial to the production of weld joint of thick section with improved metallurgical characteristics and mechanical properties along with a significant economic advantage of low cost weld edge preparation and less amount of weld deposition.

2. Experimentation

2.1 Preparation of Weld Joint

Butt weld joint using multi-pass P-GMA welding of 25-mm-thick control-rolled micro-alloyed HSLA steel plate of grade SAILMA-410HI/SA533 was prepared by MPSSPL-ENG and MPMSPL-CG welding procedure using weld deposition from 1.2-mm-diameter AWS A5.18:ER 70S filler wire in the respective weld grooves as schematically shown in Fig. 1(a) and (b). The welding was done with the polarity of direct current electrode positive (DCEP). The chemical compositions of the base plate and filler wire are shown in Table 1. During welding, the plates were rigidly fixed in a fixture as shown in Fig. 2 to minimize distortion of the joint. The weld deposition was carried out in flat position with the help of a welding torch mounted on automatically moving trolley. The welding in conventional groove (CG) was carried out by placing the torch with a narrow nozzle at required angle of attack to the groove wall, whereas the welding in extra narrow groove (ENG) was performed by a vertically placed centrally located welding torch laying a concentric weld deposition in the weld groove.

During welding, the standoff distance between the nozzle and work piece was maintained within 16-17 mm. A relatively higher electrode extension has been used to facilitate torch manipulation in the extra narrow weld groove for weld deposition with satisfactory root and groove wall fusion. Welding was carried out at different pulse parameters using commercial pure argon (99.98%) as shielding gas at a flow rate of 18 l/min. The preheating and inter pass temperature was kept in the range of 120-150 °C. The arc voltage (V) and heat input (Ω) were kept constant at 28 ± 1 V and 13.4 ± 0.5 kJ/cm, respectively. The Ω was estimated as $[(I_m \times V)/S]$ where, S is the welding speed. The pulse characteristics such as I_p , I_b , t_p , t_b and f were measured with the help of a transient recorder (maximum resolution 1 MHz) fitted with the electrical circuit of the welding set up. The shrinkage was measured after each weld pass at the groove opening after cooling down the joint to room temperature at different locations. The arc voltage and I_m were noted on the pulse characteristics recorded with the help of WMS 4000 software installed in a computer connected to the circuit of the welding power source. The measured arc voltage and mean current, I_m , at different pulse parameters giving rise to varying ϕ considered in this work are presented in Table 2.

2.2 Metallographic Studies

The transverse sections of the weld joints were polished by standard metallographic procedure and etched with 2% nital solution. Metallographic studies under optical microscope were carried out for each weld deposit and reheat-refined region of the weld passes. The microstructure of the weld has been analyzed by measuring proportional content of columnar or coaxial dendrite and equi-axed grain reheat-refined region. The dendrite fraction measurement was carried out with the help of Axio vision software-based image analyzer facility, connected with the optical microscope. The image analysis was carried out on at least 21 randomly selected spots on weld joints.

Studies on heat-affected zone (HAZ) of the base metal adjacent to fusion line were carried out on the transverse section of metallographically prepared and etched specimens of the weld joints. The studies were carried out under optical microscope on the HAZ at both sides of the weld. The width of

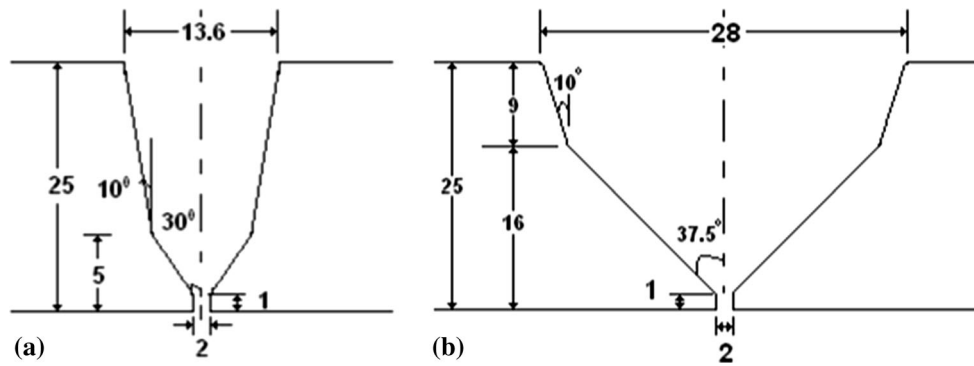


Fig. 1 Schematic diagram of (a) Extra narrow groove (ENG) and (b) Conventional V-groove (CG)

Table 1 Chemical composition of base plate and filler wire

Materials	Grade	Chemical composition (wt. %)												
		C	Si	Mn	Cr	Cu	Nb	Ti	V	Al	P	S	CE	
Base Plate 25 mm Thick (TC)	SAILMA - 410HI/SA543	0.14	0.26	1.48	...	0.02	0.41	0.024	0.010	0.015	0.024	0.010	0.39	
Base Plate 25 mm Thick (SEOS)	SAILMA - 410HI/SA543	0.13	0.32	1.35	0.01	0.02	0.04	0.020	0.048	0.013	0.032	0.007	0.40	
Filler Wire 1.2 mm, dia, (TC)	A5.18: ER 70S-6	0.1	0.9	1.6	...	0.2	0.02	0.02	0.38	

TC test certificate, SEOS Spark emission optical spectroscopy

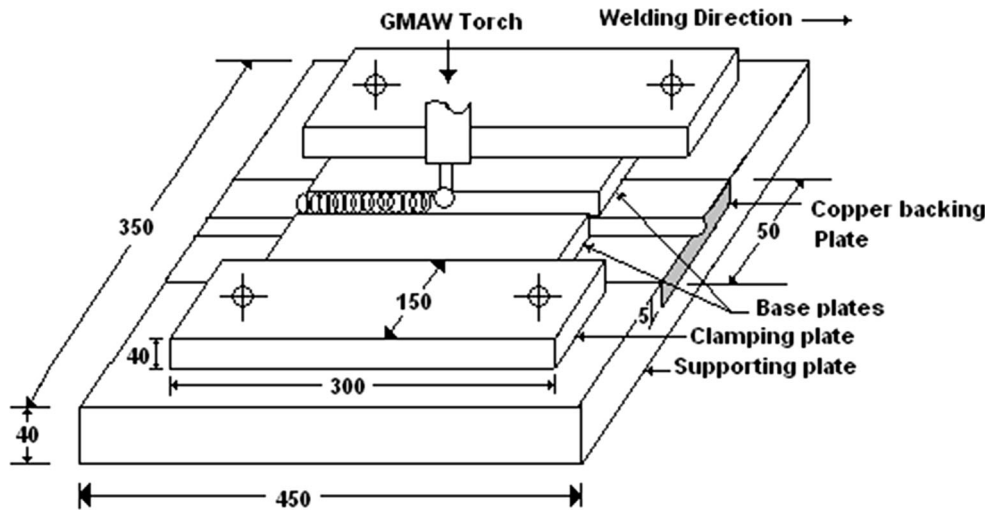


Fig. 2 Schematic diagram of welding fixture

Table 2 Welding parameters used in preparation of weld joints

Welding processes	Arc voltage, V	Heat input (Ω), kJ/cm	Welding speed (S), cm/min	Mean current $I/(I_m)$, A	ϕ	Pulse parameters				
						I_p	I_b	f , Hz	t_b , s	t_p , s
P-GMAW	28 ± 1	10.2 ± 0.4	25.5	220 ± 3	0.24	295	164	105	3.50	4.08
			27.8	240 ± 4	0.15	350	121	125	3.47	3.17
		10.2 ± 0.4	27.8	0.25	316	164	125	3.84	3.01	
			13.4 ± 0.5	21.1	0.15	350	121	124	3.47	3.17
		21.1		0.25	316	164	125	3.84	3.01	
		13.4 ± 0.5	23.2	265 ± 4	0.08	393	75	145	2.66	3.27
			23.2	0.15	360	146	145	2.97	2.98	
			23.2	0.25	328	195	145	2.55	2.88	

HAZ perpendicular to the fusion line was measured at several places on the captured images in computer with the help of Adobe Photoshop 7.0 software.

2.3 Studies on Mechanical Properties

Tensile properties of the base metal and weld joints, such as the yield strength (YS), ultimate tensile strength (UTS), and percentage elongation (Ref 12), were studied using round tensile test specimens satisfying the ASTM E8M standard. Tensile properties of weld joint were studied by using specimens machined out from axial weld (joint placed at center of the gauge length). However, the tensile properties of all weld metal were studied by machining out the specimens from the weld as shown in Fig. 3. Fracture surface of the all weld tensile specimens was examined under scanning electron microscope.

The impact toughness of weld was determined by testing Charpy V-notch (C_v) specimen at temperature of $-30\text{ }^\circ\text{C}$. The specimen of square cross section ($10 \times 10\text{ mm}$) confirming the ASTM E23 standard was machined out from central part of the weld (Fig. 4).

The micro hardness of the weld joints across the weld and HAZ was measured by Vickers micro hardness testing of Leitz Wetzlar Germany at a load of 100 grams having provision of magnification of image up to $500\times$. Prior to measuring the hardness, the specimen were polished using standard metallographic procedure and etched with 2% nital solution.

3. Results and Discussion

The use of pulse parameters according to model analysis (Ref 4) based on thermal and geometrical aspects of weld pool, allows the production of sound 25-mm-thick MPSSPL-ENG weld joint using P-GMAW process. The model analysis (Ref 4) of multi-pass single-seam per layer (MPSSPL) concentric P-GMA weld deposition technique significantly guides to introduce required temperature, geometry (width and depth) and thermal distribution in molten weld pool at a given design of narrow weld groove allowing it to appropriately touch the groove walls and spread on earlier weld bead to produce a weld joint free from lack of fusion to them. At a given Ω , the isotherm of weld pool indicating the necessary temperature distribution across its width and touching the groove wall to produce MPSSPL narrow groove weld free from lack of groove

wall fusion, has been estimated as shown in Fig. 5(a)-(d). The figure shows that at a given Ω , the variation in pulse parameters as mean current (I_m) and ϕ significantly influences the weld isotherm. The figure reveals that the length and width of the weld isotherm relatively reduces with the increase in ϕ at a given Ω and I_m . It is further observed that the length and width of isotherm increases with the increase in I_m at a given Ω and ϕ . The reduction in length and width of the weld isotherm with the increase in ϕ at a given Ω and I_m may have primarily caused by a combined influence of significant reduction in heat transfer by the arc and molten filler metal to the weld pool with the increase in ϕ (Ref 17). The reduction in heat transfer out of molten filler metal primarily happens due to enhancement of convection, conduction and radiation heat losses during transfer of droplets from the electrode tip to the weld pool. The enhancement of heat losses may have taken place because of increase in arc length with ϕ (Ref 10, 23). The increase IN width and length of the weld isotherm with the increase IN I_m at a given Ω and ϕ are primarily governed by the increase in amount of metal deposition enhancing the heat transfer to the weld pool (Ref 22).

The weld joint of HSLA steel prepared in this work was free from lack of groove wall fusion. The primary advantage of using P-GMAW in preparation of such weld joint arises from its ability to introduce more precisely controlled geometry and thermal distribution to the weld pool during each pass of weld deposition (Ref 4). The pulse parameters of ϕ , I_m and Ω , which primarily govern the welding process, also affect the metallurgical characteristics and mechanical properties of the weld (Ref 9, 13, 19). However, this is to be well understood in the light of the ability of P-GMAW process to give rise to development of comparatively low heat buildup in weld pool largely arising out of unique control over the characteristics of arc and metal transfer along with interruption in weld metal deposition under the pulse current (Ref 14, 15). Thus, the effect of ϕ at various pulse parameters on metallurgical characteristics and mechanical properties of the weld has been primarily studied under

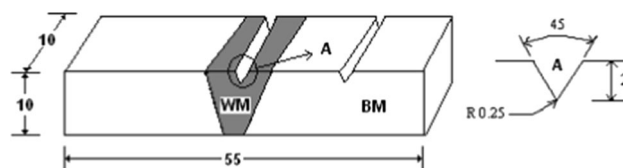


Fig. 4 Schematic diagram of the C_v - impact specimen

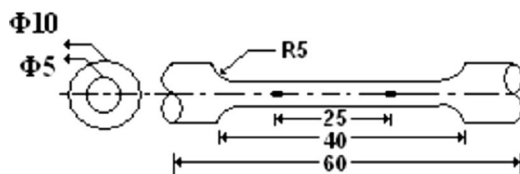
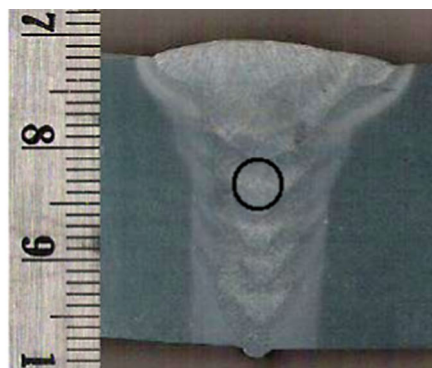


Fig. 3 Schematic diagram of the tensile specimens of all weld metal



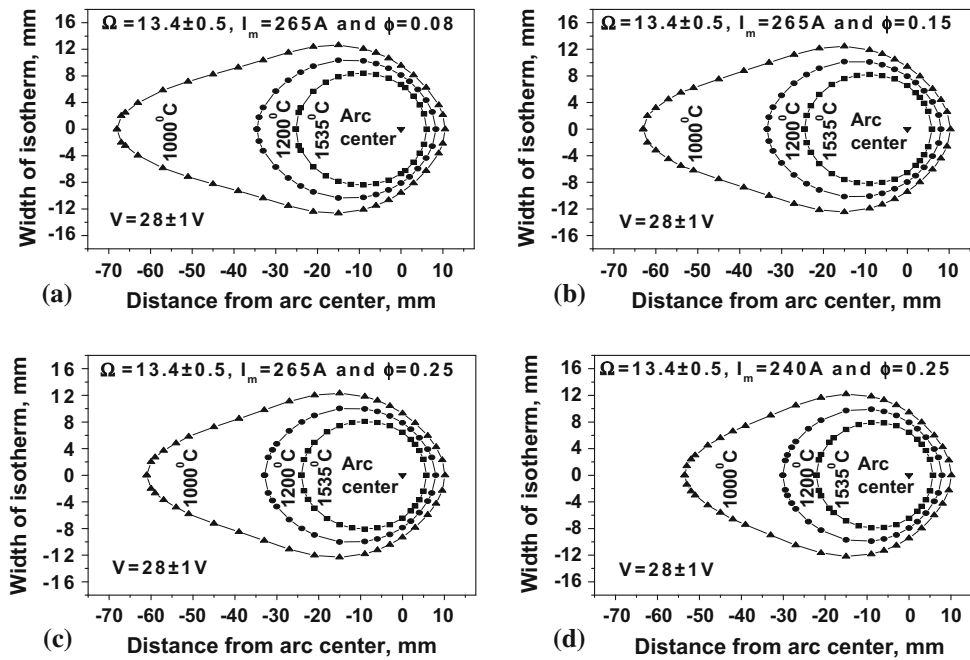


Fig. 5 At a given arc voltage and Ω typical isotherm of weld pool at different I_m and ϕ , respectively, of (a) 265A and 0.08, (b) 265A and 0.15, (c) 265A and 0.25 and (d) 240A and 0.25

given conditions of the I_m and Ω . The characteristics of MPSSPL-ENG and MPMSPL-CG weld joints prepared by using P-GMAW process under similar range of heat input have been compared. Such characteristics is governed primarily by thermal cycles and cooling rate of the weld pool which have been studied further to put more insight into it.

3.1 Thermal Cycles and Cooling Rate of Weld Pool

At a given arc voltage (V), heat input (Ω), I_m and ϕ of 28 ± 1 V, 10.2 ± 0.4 kJ/cm, 265 ± 4 A, and 0.04 in P-GMA weld deposition the typical thermal cycle showing variation of measured temperature of weld pool with time and cooling rate of it is depicted Fig. 6. This thermal cycle and cooling rate may be primarily governed by the attainment of temperature of weld pool through heat transfer to it by two sources of arc and droplet of super-heated molten filler metal. It is understood that peak temperature of weld pool reaches up to 2571 K. Therefore, the variation of total heat transferred to weld pool at different I_m and ϕ for P-GMA weld has been further studied.

At a given arc voltage of 28 ± 1 V, the influence of ϕ on heat transferred to weld pool, Q_T at different mean currents (I_m) of about 220 ± 3 , 240 ± 2 and 265 ± 4 A is depicted in Fig. 7. It is observed that the Q_T reduces with increment of ϕ at a given I_m and enhances with I_m at a given ϕ . The Q_T is primarily dictated by the arc heat, largely depending upon the effective mean current and heat of filler metal transferred per unit time, which are having similar trend of variation with ϕ at a given I_m and with I_m at a given ϕ . The empirical correlation of Q_T with ϕ and I_m at a given arc voltage have been worked out as follows.

$$Q_T = 29.19I_m - 5801.63\phi + 0.04I_m\phi + 1436.45 \quad (\text{Eq 1})$$

The Q_T may govern the temperature of weld pool (T_{WP}) affecting weld thermal cycle and cooling rate which ultimately

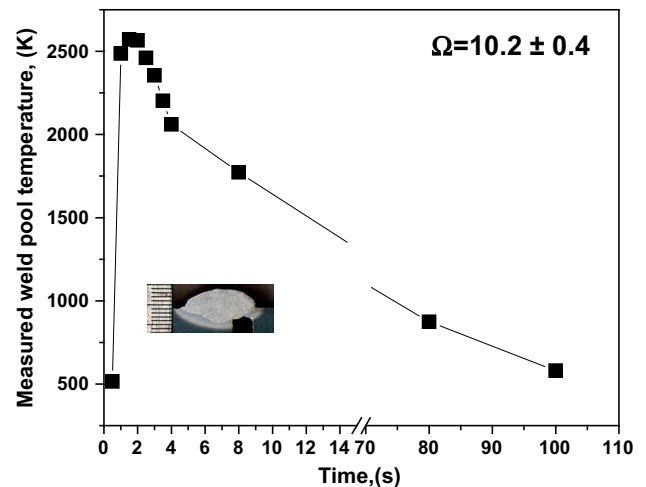


Fig. 6 Thermal cycle showing variation of measured temperature of weld pool with time and cooling rate of it for P-GMA weld deposition at a given arc voltage (V), heat input (Ω), I_m and ϕ of 28 ± 1 V, 10.2 ± 0.4 kJ/cm, 265 ± 4 A and 0.04

influences thermal behavior of weld. Thus, the thermal behavior of weld pool has been studied considering average weld pool temperature (T_{WP}) under different pulse parameters of P-GMA welding. At a given arc voltage of 28 ± 1 V the effect of ϕ on T_{WP} under different Ω is shown in Fig. 8(a)-(c). It has been understood that at a given Ω and I_m the T_{WP} reduces appreciably with increase in ϕ , it enhances with increase in Ω at a given I_m and ϕ and also increases considerably with enhancement of I_m at a given Ω and ϕ . At a given Ω and I_m , the reduction of T_{WP} with the increase in ϕ may have primarily happened due to decrease in Q_T . While, the enhancement of T_{WP} with increase in Ω at a given I_m and ϕ is accredited to increase in Q_T per unit length. However, the appreciable

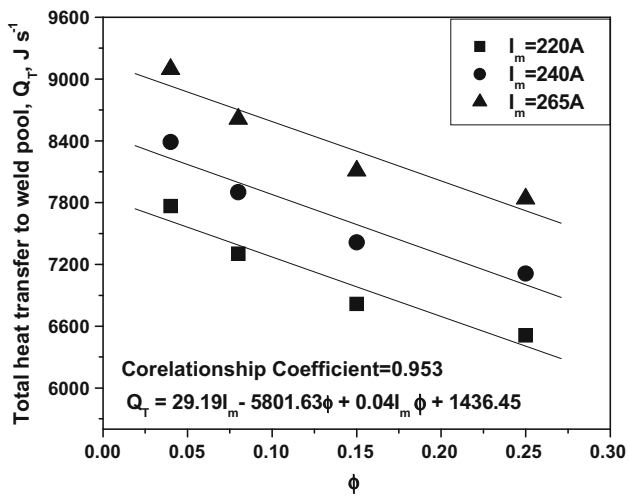


Fig. 7 At a given arc voltage of 28 ± 1 V the effect of ϕ on total heat transfer to weld pool at different I_m of 220, 240, and 265A, respectively

increment of T_{WP} with enhancement of I_m at a given Ω and ϕ has primarily happened due to increase in number of droplets transferred per pulse with the increase in I_m . This is because the molten metal droplets carry substantial amount of heat during its transfer to weld pool. The empirical correlation of T_{WP} with Ω and ϕ has been obtained as follows.

$$(T_{WP})_{220A} = 32.80\Omega - 965.55\phi + 5.84\Omega\phi + 1868.97 \quad (\text{Eq 2})$$

$$(T_{WP})_{240A} = 32.01\Omega - 1057.02\phi + 13.94\Omega\phi + 2038.62 \quad (\text{Eq 3})$$

$$(T_{WP})_{265A} = 32.62\Omega - 1023.02\phi + 10.12\Omega\phi - 2217.71 \quad (\text{Eq 4})$$

3.2 Microstructure of HSLA Steel Used for Preparation of Weld Joints

The microstructures of 25-mm-thick micro-alloyed HSLA steel plates used for preparation of weld joints are shown in Fig. 9. It has been observed that the microstructures of base metal consist of ferrite as light etching constituent and pearlite depicted by dark etching constituent along the lamination of matrix of banded structure.

3.3 Weld Appearance and Size

Weld appearance and size has been studied for both the MPMSPL-CG and MPSSPL-ENG weld joint. The observations are analyzed and compared to ascertain the superiority of MPSSPL-ENG weld joint with respect to various aspects of that of MPMSPL-CG weld joint.

3.3.1 MPMSPL-CG Weld Joint. At a given arc voltage, ϕ , I_m and Ω of 28 ± 1 V, 0.25, 265 ± 4 A, and 13.4 ± 0.5 kJ/cm, respectively, the typical macrograph of weld as revealed in transverse section of the MPMSPL-CG weld joint is shown in Fig. 10. The figure shows the soundness of weld joint with respect to lack of fusion in between the inter bead deposit and the groove wall to weld deposit.

3.3.2 MPSSPL-ENG Weld Joints. At a given close range of arc voltage and Ω of 28 ± 1 V, and 13.4 ± 0.5 kJ/cm, respectively, the typical macrographs of the weld as revealed in transverse section of the MPSSPL-ENG weld joints prepared at different mean currents (I_m) of 240 ± 2 , and 265 ± 4 A under different ϕ of 0.08, 0.15 and 0.25 are shown in Fig. 11. The figure typically reveals the uniformity of weld joints as well as their soundness primarily with respect to the presence of lack of fusion in them. The figure also shows that the size of molten weld pool per pass is appreciably smaller than that observed in case of the MPMSPL-CG weld (Fig. 10) which may impart relatively less thermal severity in the weld joint. However, no weld was prepared at the I_m and ϕ of 240 ± 2 and 0.08, respectively, as it gives significant amount of porosity in weld deposit. This is because such a low order of ϕ at relatively lower I_m results air aspiration in unstable shielding gas jacket of P-GMAW process (Ref 10).

3.4 Microstructure of Weld

The microstructure of weld deposit often plays a significant role in governing the properties of weld joint. The presence of coarse dendrites in weld metal can be considered (Ref 13) as one of the primary cause of failure of weld joint. Thus, to achieve desired properties of a multi-pass weld, a control over the coarsening of microstructure of weld metal and its proportionate presence with respect to the reheat-refined region may be quite useful. The microstructure of weld is largely governed by the chemical composition; temperature and cooling rate of weld pool. The chemical composition of weld metal is primarily dictated by compositions of the filler metal as well as the extent of dilution of base metal. In GMAW process, the degree of dilution and characteristics of weld pool primarily depends upon weld groove design and temperature of weld pool. Temperature of weld pool is governed by the process heat input, Ω , and the heat transferred to weld pool by super-heated metal droplets. The cooling rate under a given heat sink controls the solidification mechanism of weld pool as well as solid state phase transformation in weld deposit and reheat-refined region. The cooling of weld primarily takes place by transfer of heat to the base metal through conduction while other mechanisms of heat loss due to convection and radiation from the molten weld pool to the surrounding remain effective. Thus, it may be understood that the weld groove design along with the welding parameter and procedure may significantly influence the microstructure of a multi-pass weld.

The use of pulsed current GMAW process may appreciably affect the microstructure of weld metal primarily by influencing its solidification mechanism through control of weld pool temperature resulting from heat input and heat built up in it and interruption in metal deposition dictated by the pulse parameters. Accordingly various aspects of the microstructure of MPMSPL-CG and MPSSPL-ENG weld and their HAZ has been analyzed and compared in reference to the concerned welding parameters and procedures.

3.4.1 MPMSPL-CG Weld. At a given arc voltage, I_m , ϕ and Ω of 28 ± 1 V, 265 ± 4 A, 0.25 and 13.4 ± 0.5 kJ/cm, respectively, the typical microstructure of MPMSPL-CG weld deposit revealing its dendritic and reheat-refined microstructure under optical microscope is shown in Fig. 12. Microstructure of the two distinctly different regions has been found to consist of coaxial dendrite of weld deposit and fine grain morphology of reheat-refined region of the weld. The reheat-refined region

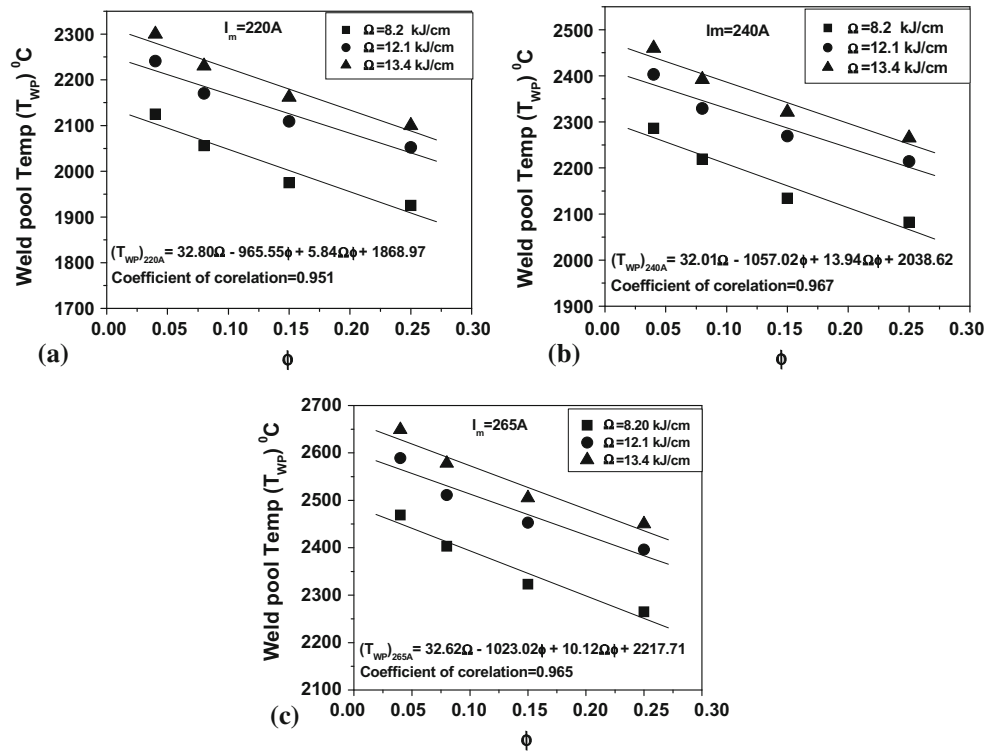


Fig. 8 At a given arc voltage of 28 ± 1 V, the effect of ϕ and Ω on weld pool temperature under different mean current of 220, 240, and 265 A, respectively

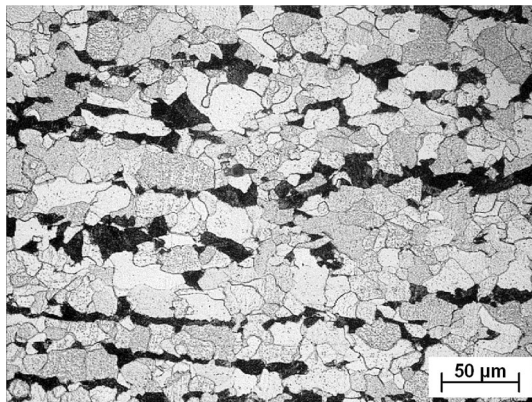


Fig. 9 Typical microstructure of 25-mm-thick HSLA steel base plate

may have primarily generated due to commonly known partial melting and heat treatment of earlier weld bead by subsequent weld deposition of multi-pass welding process. The microstructure of it largely contains ferrites and acicular ferrites of interlocking nature produced due to cooling of molten metal of weld.

3.4.2 MPSSPL-ENG Weld. At a given arc voltage (V) and Ω of 28 ± 1 V and 13.4 ± 0.5 kJ/cm, respectively, effect of ϕ and I_m on microstructure of MPSSPL-ENG centrally laid P-GMA weld deposit has been shown in the micrographs presented in Fig. 13. Similar to MPMSPL-CG weld, here also the microstructure of weld metal has been found as usual consist of a mixture of coaxial dendrite and reheat-refined region of multi-pass weld. However, their amount and distribution in the multi-pass welds are found to vary with a change

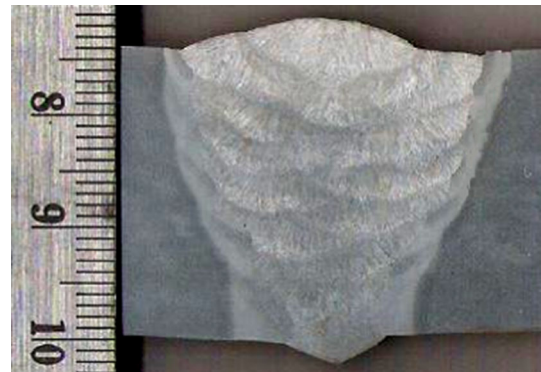


Fig. 10 Typical macrograph of MPMSPL-CG P-GMA weld joint at a given arc voltage and Ω of 28 ± 1 V and 13.4 ± 0.5 kJ/cm and ϕ , I_m of 0.25, 265A

in welding parameters as I_m and ϕ . Also in MPSSPL-ENG centrally laid welding procedure, the variations in microstructural aspects of weld deposits are as usual primarily governed by the extent of partial re-melting and reheat refinement of dendritic microstructure of an earlier deposited weld bead by a later one. But the fraction of different microstructure content of the matrix varies with the pulse parameters due to their significant influence on geometry and thermal characteristics of weld bead (Ref 17). At the same time, the microstructure of weld mainly consists of ferrites and acicular ferrites resulted out of cooling of molten metal of weld deposit.

The variation in fraction of coaxial dendritic region and reheat-refined region of weld deposit with the change in I_m and ϕ at a given Ω of 13.4 ± 0.5 kJ/cm, is shown in Fig. 14 and 15, respectively. It has been observed that fraction of dendritic

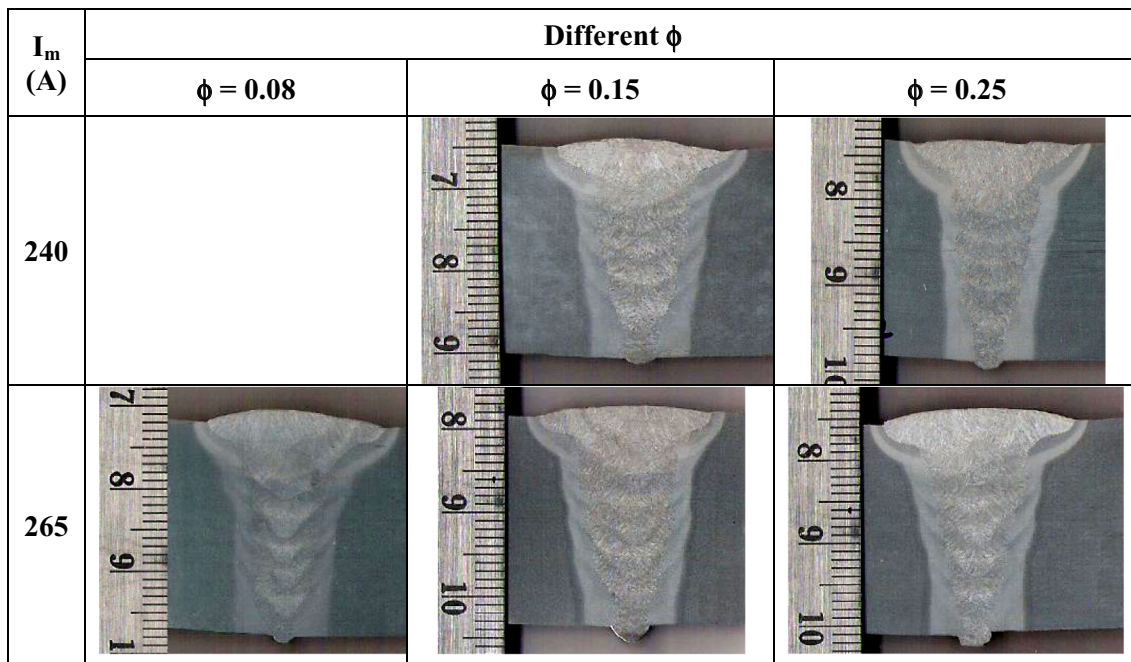


Fig. 11 Typical macrographs of MPSSPL-ENG P-GMA weld joints at a given arc voltage and Ω of 28 ± 1 V and 13.4 ± 0.5 kJ/cm, respectively, under different ϕ and I_m

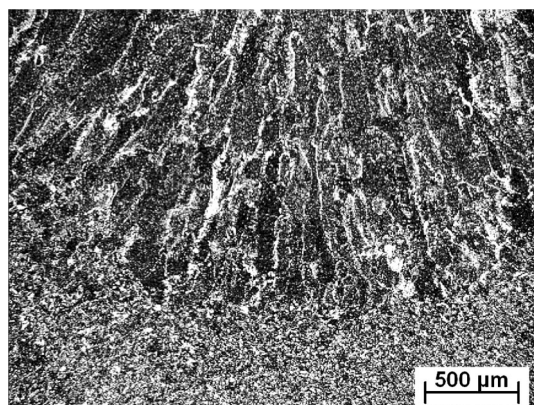


Fig. 12 Typical microstructure from central part of a MPMSPL-CG P-GMA weld prepared at an arc voltage, ϕ , I_m and Ω of 28 ± 1 V, 0.25 and 265A and 13.3 ± 0.4 kJ/cm respectively

region of weld deposit is comparatively higher and consequently the reheat-refined region is relatively lower in case of MPMSPL-CG weld than that of the MPSSPL-ENG weld at a given I_m and ϕ . This may be primarily attributed to application of comparatively lower amount of weld deposition per unit length contributing to a more uniform and wider thermal distribution in reheat refinement at MPSSPL-ENG weld. It is further understood that at a given Ω and I_m , the increase in ϕ enhances the dendrite fraction and consequently reduces the fraction of reheat-refined region in the MPSSPL-ENG weld, while at a given Ω and ϕ , the increase in I_m decreases the dendrite fraction and increases the reheat refinement fraction. At a given Ω and I_m , the enhancement of dendritic fraction and consequent reduction in reheat refinement fraction in the MPSSPL-ENG weld with the increase in ϕ may be primarily attributed to relatively lower weld pool temperature (Ref 6) and smaller amount of weld metal deposition per unit length (Ref

18) resulting in lower thermal impact. Such a variation of dendritic as well as reheat-refined fraction with the increase in I_m may have also largely happened due to combined influence of total heat transferred (Ref 16, 17) to weld pool and amount of metal deposition (Ref 18) per unit length at a given Ω and ϕ .

At a given similar range of arc voltage and Ω , the effect of variation in ϕ and I_m on overall characteristics of dendritic matrix in the MPMSPL-CG weld and the MPSSPL-ENG weld is shown in Fig. 16. The morphology of various constituents of microstructure of all the weld deposits, as revealed at comparatively higher magnification, is shown in Fig. 17. The weld metal begins their solidification by formation of δ ferrite from molten state. Upon further cooling to room temperature, the δ ferrite transforms into two phases. At higher temperature, δ ferrite transforms to austenite while at lower temperature it is converted to different forms of ferrites of α ferrite and acicular ferrite. It can be understood that the observed microstructure of weld at all I_m and ϕ may primarily consists of α ferrite and acicular ferrite. The temperature of the weld pool is high enough to dissolve a considerable amount of oxygen. The extent of dissolution of oxygen is governed by thermodynamic properties of weld pool, gas and chemical composition of weld. According to chemical analysis of the filler wire (Table 1), it is observed that the filler wire contain relatively higher amount of manganese and silicon as compared to base material used in preparation of weld joint. At a given Ω and I_m , the dilution decreases with increase in ϕ . Therefore, the content of manganese and silicon in the weld will be relatively higher at elevated ϕ resulting in higher percentage of oxides of these metals. The oxides of manganese and silicon act as potent inclusion working as nucleation sites of acicular ferrite and promoting its formation in the matrix. Thus, it can be inferred that the amount of acicular ferrite increases with the increase in ϕ . In addition to this, an increase in I_m increases the dilution resulting in availability of comparatively lesser amount of manganese and silicon in weld. This may result in relatively

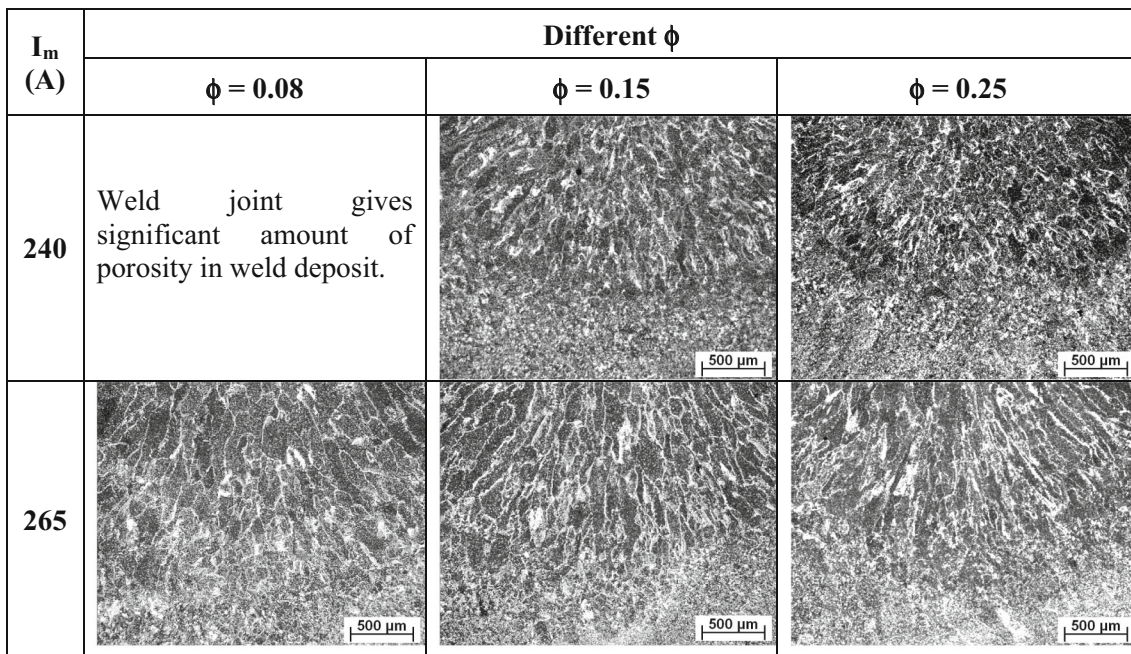


Fig. 13 At a given arc voltage and Ω of 28 ± 1 V and 13.4 ± 0.5 kJ/cm typical microstructures of central part of MPSSPL-ENG P-GMA weld prepared at different I_m and ϕ

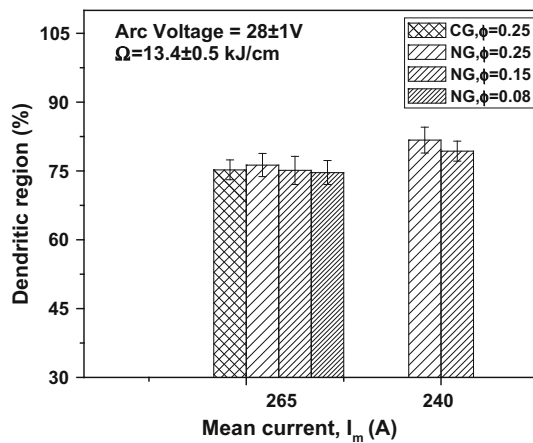


Fig. 14 Effect of I_m and ϕ on percentage of dendritic region of MPMSPL-CG and MPSSPL-ENG P-GMA weld prepared at a given arc voltage and Ω of 28 ± 1 V and 13.4 ± 0.5 kJ/cm, respectively

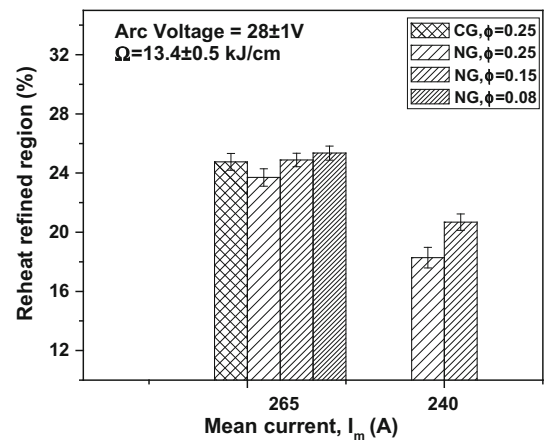


Fig. 15 Effect of I_m and ϕ on percentage of reheat-refined region of MPMSPL-CG and MPSSPL-ENG P-GMA weld prepared at a given arc voltage and Ω of 28 ± 1 V and 13.4 ± 0.5 kJ/cm, respectively

less formation of oxides of these elements in the weld giving rise to reduction of acicular ferrite with the increase in I_m . It is further noted that at a given I_m and ϕ the microstructure of MPSSPL-ENG weld is relatively finer as compared to that of the MPMSPL-CG weld possibly because a comparatively narrower distribution of weld thermal intensity (Fig. 5) prevails in the former one due to comparatively lower amount of weld deposition per pass (Fig. 7). It is also observed that at a given Ω and I_m , the microstructure of weld deposit becomes relatively finer with the increase in ϕ . This has primarily happened because of generation of comparatively lower weld pool temperature resulting in higher cooling rate and reduction of area of weld deposit with the increment of ϕ (Ref 6). However, the figure also depicts that at a given Ω and ϕ , the increase in I_m coarsens the microstructure of weld deposit due to increase in T_{WP} and relatively lower cooling rate of weld pool (Ref 7).

At a given arc voltage and Ω , the variations in morphology of reheat-refined microstructures in the MPMSPL-CG and MPSSPL-ENG weld considered as heat-affected zone of earlier deposited weld (HAZ), as revealed at relatively higher magnification, are shown in Fig. 18. The figure shows that at a given I_m and ϕ microstructure of reheat-refined zone is comparatively finer in the MPSSPL-ENG weld as compared to that observed in the MPMSPL-CG weld deposit because of the presence of comparatively narrower distribution of heat in weld and lower thermal impact largely due to relatively smaller weld deposition per pass in the former one as discussed earlier. The microstructure primarily consists of again α ferrite and acicular ferrite, but the extent of acicular ferrite is comparatively higher as compared to dendrite matrix of the weld at all ϕ and I_m . The proportion of acicular ferrite in the reheat-refined

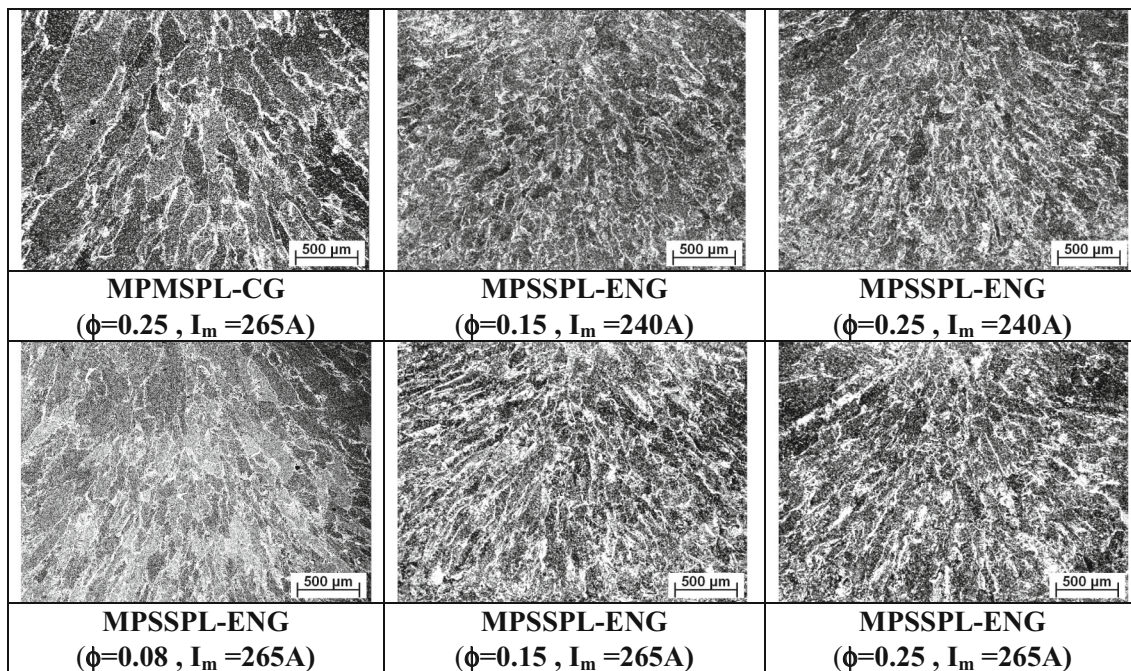


Fig. 16 Typical dendritic microstructures of MPMSPL-CG and MPSSPL-ENG P-GMA weld prepared at different I_m and ϕ

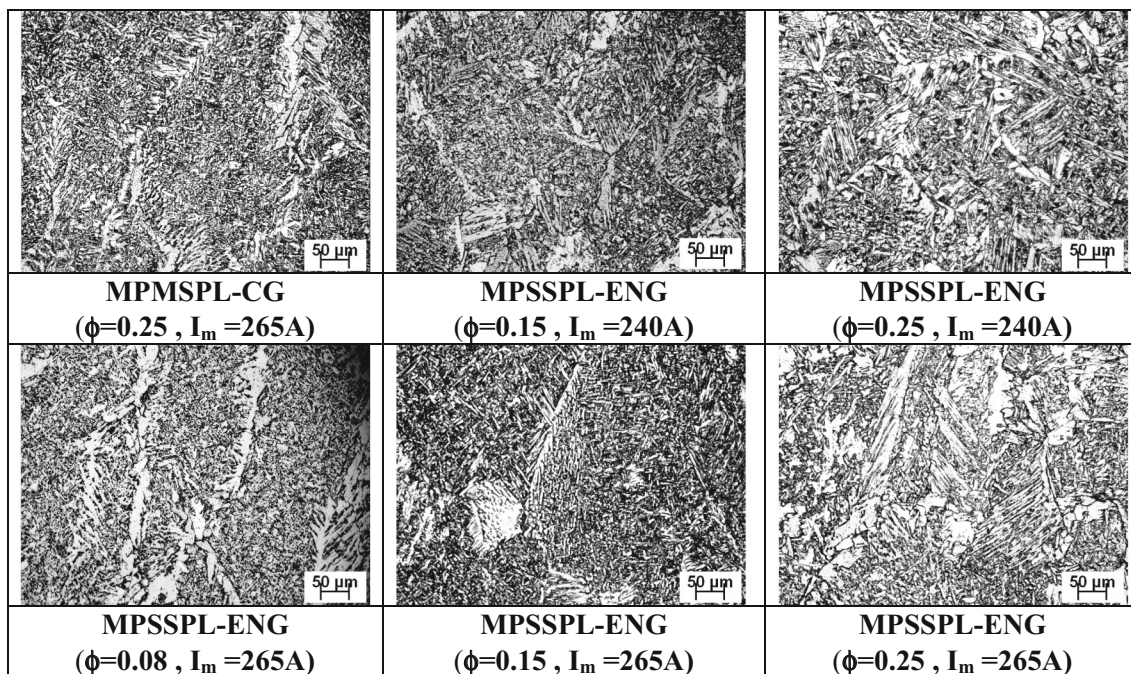


Fig. 17 Typical dendritic microstructures of MPMSPL-CG and MPSSPL-ENG P-GMA weld at comparatively higher magnification prepared at different I_m and ϕ

zone of weld enhances with increase in ϕ at a given I_m and Ω , whereas the proportion of α ferrite reduces with increase in ϕ at a given I_m and Ω . Again it is observed that the acicular ferrite in reheat-refined zone of the weld reduces and α ferrite enhances with increase in I_m . This observation may be in line with variation in impact toughness of the weld where, increase in acicular ferrite and decrease in α ferrite enhances the impact toughness which has been studied further. The figure also depicts that with the increase in ϕ and decrease in I_m at a given

Ω , the microstructure becomes finer possibly due to lower heat transfer to the weld pool giving rise to relatively lower temperature it along with its faster cooling (Ref 6).

3.5 Studies on HAZ

At a given arc voltage, I_m , ϕ and Ω of 28 ± 1 V, 265 A, 0.25, and 13.4 ± 0.5 kJ/cm, respectively, the typical nature of extent of heat-affected zone (HAZ) influencing the microstruc-

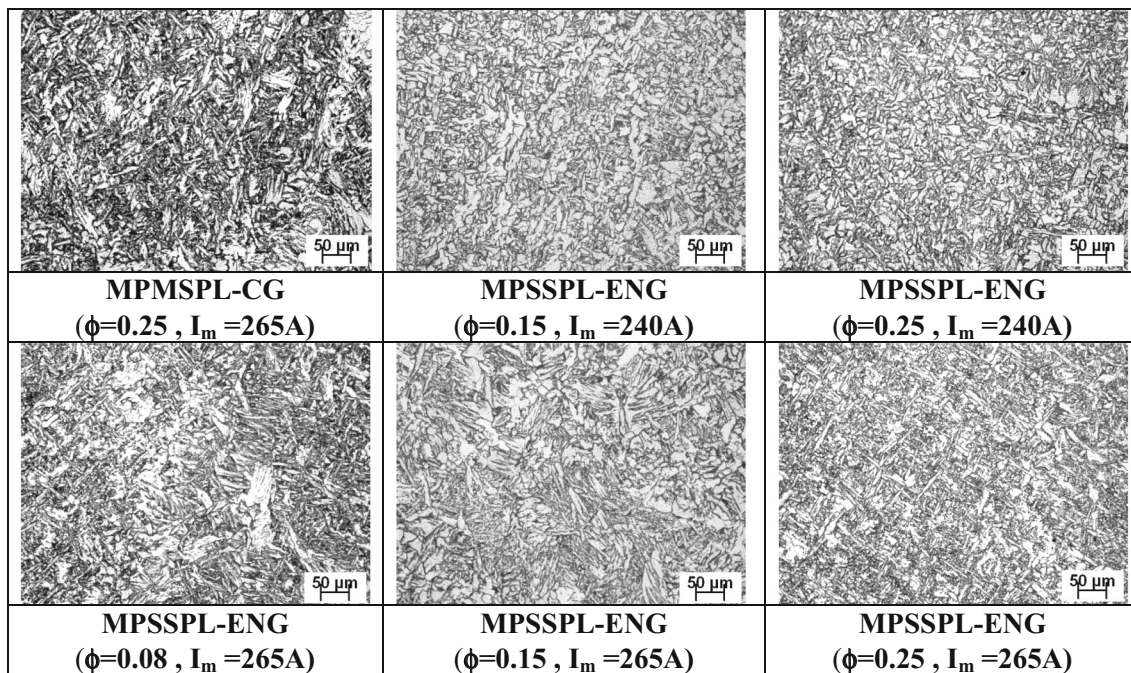


Fig. 18 Typical reheat-refined microstructure of MPMSPL-CG and MPSSPL-ENG P-GMA weld prepared at different I_m and ϕ

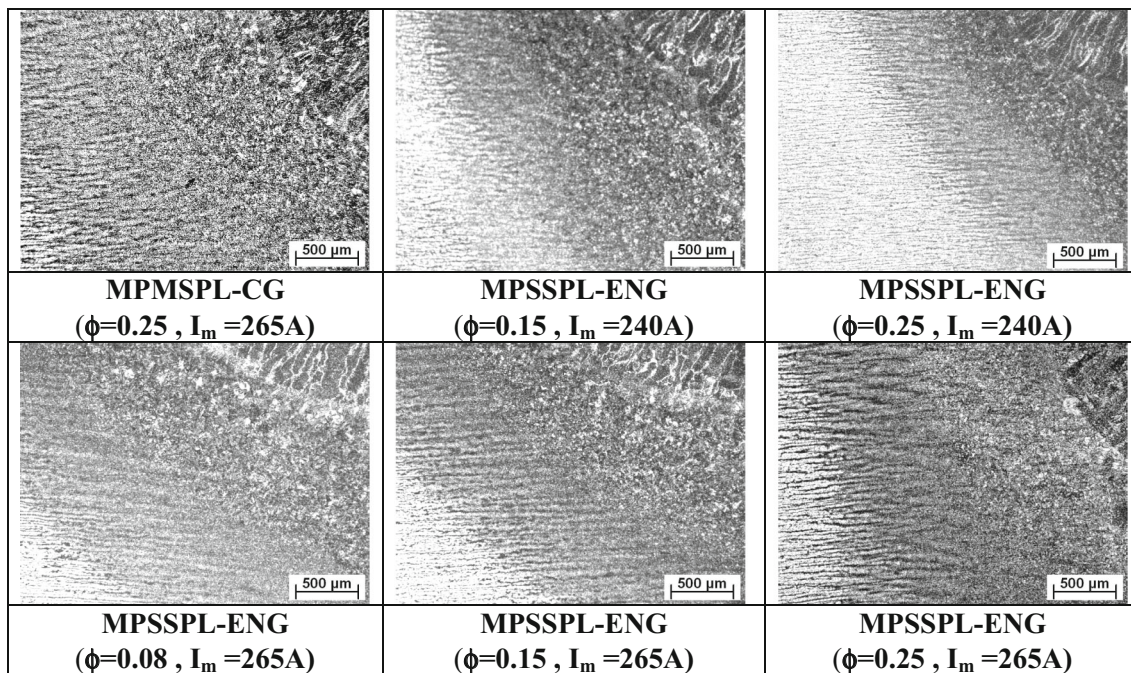
ture of base metal close to fusion line of the MPMSPL-CG weld joint is shown in Fig. 19(a). Morphology of this region revealed at comparatively higher magnification is also shown in Fig. 19(b). Similarly at the given arc voltage and Ω of 28 ± 1 V and 13.4 ± 0.5 kJ/cm respectively, the influence of I_m and ϕ on the extent of HAZ affecting the microstructure of base metal close to fusion line of the MPSSPL-ENG weld joints is also shown in Fig. 19(a). The figure shows that the microstructure of HAZ becomes comparatively coarser as one goes closer to the fusion line. The microstructure of HAZ of all weld joints of MPMSPL-CG weld and MPSSPL-ENG weld becomes finer as one goes away from fusion line. The temperature of base metal in HAZ due to heat of welding increases above critical temperature in austenitic range. Upon cooling, there may be formation of proeutectoid ferrite initially but later on because of comparatively higher cooling rate prevailing, austenite transformed into combination of acicular ferrite and pearlite. The acicular ferrite and pearlite observed in HAZ of base metal of HSLA steel has been observed to be relatively lower as compared to HAZ of earlier deposited weld but it is higher relative to that observed in dendrite matrix of weld. It is observed that the extent of acicular ferrite and pearlite increases with enhancement of ϕ at a given I_m and Ω . The acicular ferrite decreases with increases of I_m at a fixed value of ϕ and Ω . It can be further said that the proeutectoid ferrite reduces with increase in ϕ at a given I_m and Ω , and enhances with I_m . Also the HAZ microstructure of MPMSPL-CG weld joint has been found significantly coarser than that of the HAZ of MPSSPL-ENG weld joint prepared at any pulse parameters. It also appears that at a given Ω and I_m , the increase in ϕ and at a given Ω and ϕ , the decrease in I_m relatively reduces the width of HAZ. This may have primarily happened because the increase in ϕ and decrease in I_m reduces heat transfer to the weld pool (Ref 17) as it is also reflected in shrinkage of the size of weld isotherm (Fig. 5). In view of this, the severity of HAZ changing the microstructure of base metal has been character-

ized by measuring its width and the size of coarse grain in the matrix adjacent to fusion line. At a given arc voltage and Ω of 28 ± 1 V and 13.4 ± 0.5 kJ/cm, respectively, the effect of I_m and ϕ on the width of HAZ in MPSSPL-ENG weld joint is shown in Fig. 20. The results show that at a given Ω and I_m , the width of HAZ decreases with the increase in ϕ . The figure also depicts that at a given Ω and ϕ , the increase in I_m appreciably increases the width of HAZ. The variation in width of HAZ with the change in I_m and ϕ may be primarily attributed to the variation in heat transfer to the weld pool as well as width and length of weld isotherm (Fig. 5), as it is also reported elsewhere (Ref 4) in detail.

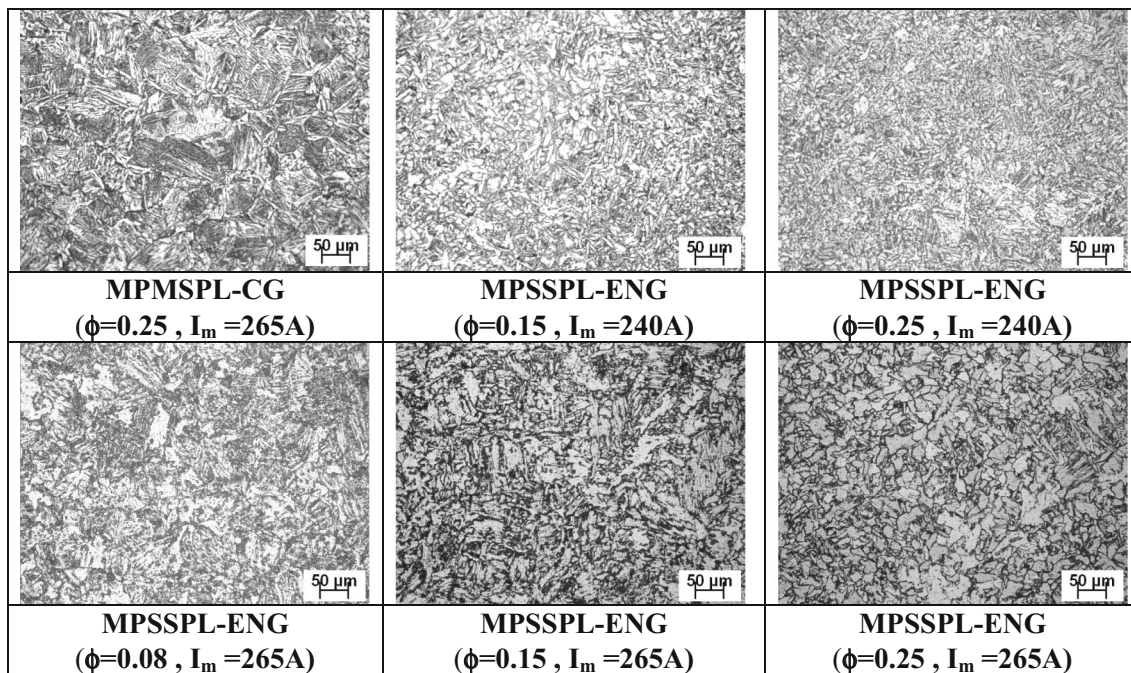
At a given arc voltage and Ω of 28 ± 1 V and 13.4 ± 0.5 kJ/cm, respectively, effect of I_m and ϕ on grain coarsening in HAZ adjacent to fusion line of the MPMSPL-CG and MPSSPL-ENG weld joints is shown in Fig. 21. It is observed that the grain size in case of MPMSPL-CG weld joint is comparatively higher than that of MPSSPL-ENG centrally laid P-GMA weld joint. The figure also reveals that at a given Ω and I_m , the increase in ϕ appreciably reduces the grain size adjacent to fusion line. It is further observed that at a given Ω and ϕ , the increase in I_m increases the grain size adjacent to fusion line. In agreement to earlier discussions, the change in grain size as a function of I_m and ϕ may have also been attributed to variation in severity of thermal behavior of the weld where, a comparatively lower amount of metal deposition per unit length in MPSSPL-ENG weld joint results in relative lowering of thermal severity.

3.6 Tensile Properties

Tensile properties of the weld joint have been studied for both the axial and all weld specimens in order to characterize it in reference to those of the base material. The properties are analyzed considering the yield strength, ultimate tensile strength, and elongation of the weld joints.



(a)



(b)

Fig. 19 Typical microstructures of HAZ of MPMSPL-CG and MPSSPL-ENG P-GMA weld joints at a given arc voltage and Ω of 28 ± 1 V and 13.4 ± 0.5 kJ/cm of varied I_m , ϕ at relatively (a) low and (b) high magnifications

3.6.1 Axial Weld. The location of fracture in the axial tensile specimens of the MPMSPL-CG and MPSSPL-ENG weld joints is typically shown in Fig. 22(a)-(f). The figure depicts that the fracture always occurs away from the weld and it is mostly confined to the base metal irrespective of the type of weld joint and welding parameters used. Thus, it may be understood that tensile strength of the weld always remains relatively higher than that of the base metal irrespective of the welding parameters and procedure used.

3.6.2 All Weld. At a given arc voltage and Ω of 28 ± 1 V and 13.4 ± 0.5 kJ/cm, respectively, the effect of I_m and ϕ on yield strength, ultimate tensile strength, and elongation of all weld specimens of the MPMSPL-CG and MPSSPL-ENG weld joints is shown in Fig. 23, 24 and 25 respectively. A higher tensile property by about 10-27% generally has been observed in case of MPSSPL-ENG weld in comparison with that of the MPMSPL-CG weld. Such a variation in tensile properties of the welds is primarily attributed to the changes in microstruc-

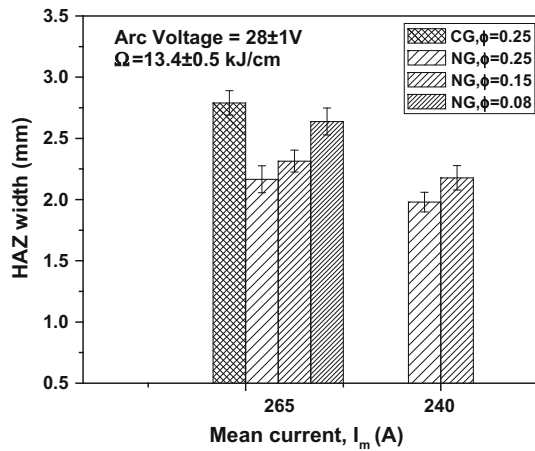


Fig. 20 Effect of I_m and ϕ on HAZ width of MPMSPL-CG and MPSSPL-ENG P-GMA weld joints prepared at a given arc voltage and Ω of 28 ± 1 V and 13.4 ± 0.5 kJ/cm, respectively

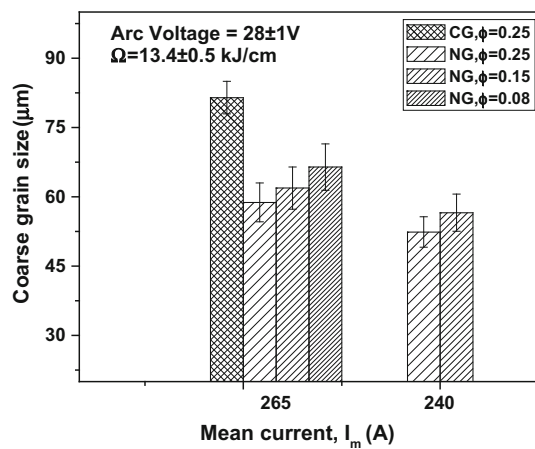


Fig. 21 Effect of I_m and ϕ on coarse grain size adjacent to fusion line of MPMSPL-CG and MPSSPL-ENG P-GMA weld joints prepared at a given arc voltage and Ω of 28 ± 1 V and 13.4 ± 0.5 kJ/cm, respectively

ture as being finer in MPMSPL-CG weld as compared to MPSSPL-ENG weld. Also, it is governed by variation of microstructure relative content of reheat-refined zone as discussed earlier. It is observed that at a given Ω and I_m , the yield strength (YS), and ultimate tensile strength (UTS) increases but percentage elongation decreases with the increase in ϕ . It is also observed that at a given Ω and ϕ , the increase in I_m appreciably reduces the yield strength (YS) and ultimate tensile strength (UTS) but enhances the percentage elongation. Such a variation of tensile properties with respect to I_m and ϕ may have primarily happened again due to changes in fraction of dendritic and reheat-refined regions in the matrix where, a decrease in reheat-refined region (Fig. 15) primarily enhances the strength but, reduces elongation of the weld. However, this behavior has been found true in case of variation in ϕ at a given I_m but not so in case of variation of I_m at a given ϕ . This is because the predomination of dendrite fraction on mechanical properties is also further attributed to its morphology (Fig. 17) dictated by the pulse parameters as discussed above where, the refinement of dendrite and, presence of interlocking acicular ferrite improves the properties. The fractured surfaces of all

weld tensile specimens of the MPMSPL-CG weld and MPSSPL-ENG weld prepared at different pulse parameters used under a given Ω are shown in Fig. 26. The figure reveals that mode of fracture of the weld is largely ductile in nature characterized by the formation of dimples.

3.7 Charpy Impact Toughness

At a given arc voltage, Ω , I_m and ϕ of 28 ± 1 V, 13.4 ± 0.5 kJ/cm, 265 A and 0.25, respectively, the C_V impact toughness at -30°C of the MPMSPL-CG weld has been compared to that of the MPSSPL-ENG weld prepared at the same arc voltage, Ω with different I_m and ϕ as shown in Fig. 27. The fractured specimens in both the cases are found to be significantly deformed in dimension during fracture under impact loading confirming ductile nature of the weld. It has been observed that the MPSSPL-ENG weld prepared at different welding parameters has about 12-39% higher impact toughness than that of the MPMSPL-CG weld. It is further observed that at a given Ω and I_m , the impact toughness increases with the increase in ϕ and at a given Ω and ϕ , it increases with the decrease in I_m . This is in reference to Fig. 15 where it may be noted that the reduction in fraction of reheat-refined region increases the impact toughness of the weld. Thus, it may be assumed that the toughness of weld is predominantly governed by the coaxial dendrite fraction and its morphology in weld deposit. In this regard, it is understood that the presence of finer dendrite microstructure along with transformation of relatively higher amount of acicular ferrite responsible for higher impact toughness (Fig. 13) improves the toughness of the weld. The interlocking nature of acicular ferrite, together with its fine grain size, provides maximum resistance to crack propagation and consequently improves the impact toughness (Ref 20, 21). It can be understood that enhancement of impact toughness with the increase in ϕ may be due to increase in amount of acicular ferrite with ϕ . Further, it can be said that the reduction of impact toughness with increase in I_m can be because of reduction in acicular ferrite with increases of I_m as discussed in section 3.4.2.

The SEM views of the fracture surface of Charpy impact test specimen are shown in Fig. 28. The fractograph of all the specimens reveals mixed mode of fracture depicting the presence of dimpled morphology and cleavage characterizing the ductile and brittle behavior of fracture respectively. However, the fractograph of MPMSPL-CG weld qualitatively shows the presence of relatively higher area fraction of ductile fracture as compared to that observed in the fractograph of the MPSSPL-ENG weld. This may be understood in the light of the earlier discussions on comparatively higher severity of thermal behavior of the MPMSPL-CG weld than that of the MPSSPL-ENG weld affecting their microstructure. Similarly at a given Ω and I_m , the increase in ϕ and at a given Ω and ϕ , the decrease in I_m appreciably reduces the area fraction of brittle fracture allowing relatively more domination of ductile fracture. Such a variation of area fraction of ductile and brittle fracture on the fracture surface with respect to I_m and ϕ may have happened due changes in heat transferred to the weld pool as discussed above.

3.8 Hardness Studies

The hardness distribution across the weld joint has been studied primarily to understand the response of the material to weld thermal behavior resulting from different welding param-

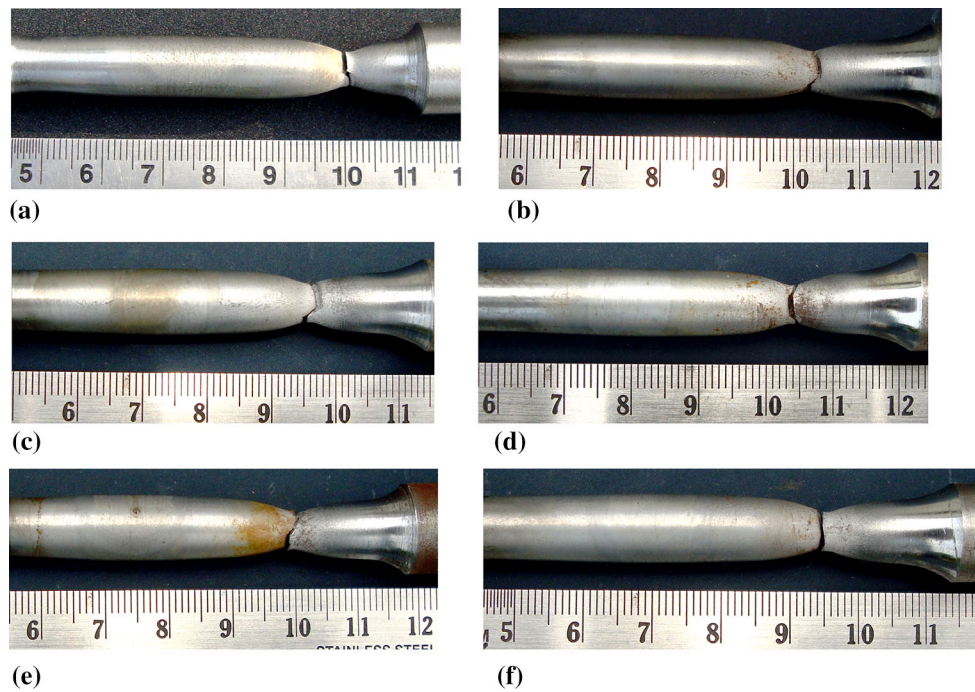


Fig. 22 Typical location of fracture under tensile loading on axial weld test of MPMSPL-CG and MPSSPL-ENG P-GMAweld joints at different ϕ and I_m of (a) CG, 0.25 and 265A (b) NG, 0.15 and 240A, (c) NG, 0.25 and 240A, (d) NG, 0.08 and 265A, (e) NG, 0.15 and 265A and (f) NG, 0.25 and 265A

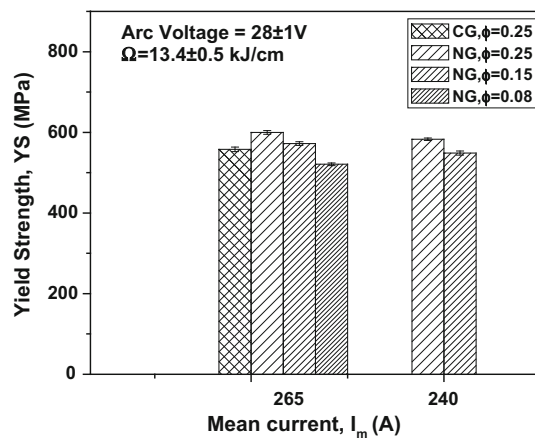


Fig. 23 Effect of I_m and ϕ on yield strength of MPMSPL-CG and MPSSPL-ENG P-GMA weld joints prepared at a given Ω of 13.4 ± 0.5 kJ/cm

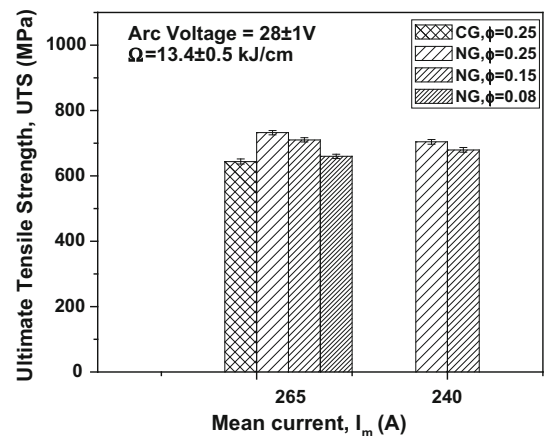


Fig. 24 Effect of I_m and ϕ on ultimate tensile strength of MPMSPL-CG and MPSSPL-ENG P-GMA weld joints prepared at a given Ω of 13.4 ± 0.5 kJ/cm

eters and affecting the properties of different zones of weld joint based on their morphology characterizing the quality of the weld joint. Hardness distribution across the weld joint prepared at a given arc voltage and Ω of 28 ± 1 V and 13.4 ± 0.5 kJ/cm, respectively, has been compared for MPMSPL-CG weld and MPSSPL-ENG weld in Fig. 29. It is broadly observed that the hardness of weld deposit in MPSSPL-ENG weld is relatively higher than that found in the MPMSPL-CG weld. But, in spite of relatively more grain coarsening in the HAZ close to fusion line (FL) of the MPMSPL-CG weld joint (Fig. 14), its hardness has been found

relatively higher than that found in the similar region of HAZ of the MPSSPL-ENG weld joint. It shows that the hardness of this region of HAZ is predominantly governed by its phase transformation than grain coarsening. This is in agreement to the microstructure of the weld and HAZ of the two classes of weld joints as discussed above with respect to their thermal behavior. However, it appears that at a given I_m , lowering of ϕ and at a given ϕ , lowering of I_m relatively reduces the hardness of HAZ close to FL in the MPSSPL-ENG weld joint. Certain amount of scattering in hardness distribution across the weld may have primarily occurred due to random indentation at

different zones of microstructure having dendrite and reheat-refined morphology. However, as one goes away from the FL the hardness decrease rapidly depending upon the width of HAZ.

4. Conclusions

At a given arc voltage and heat input of pulse current gas metal arc welding (P-GMAW), the use of multi-pass single-seam per layer extra narrow gap (MPSSPL-ENG) by

centrally laid weld deposition gives rise to comparatively finer microstructure of weld and HAZ than that of the weld joint of thick HSLA steel plate prepared by multi-pass multi-seam per layer conventional groove (MPMSPL-CG) technique. In case of all the ENG and CG weld joints the tensile strength of weld and HAZ has been found relatively higher giving rise to fracture from base metal in axial weld test. The tensile and C_v impact toughness properties of the MPSSPL-ENG weld are always been found to be superior to those of the MPMSPL-CG weld where the extent of improvement in properties of the former one significantly depends upon pulse parameters.

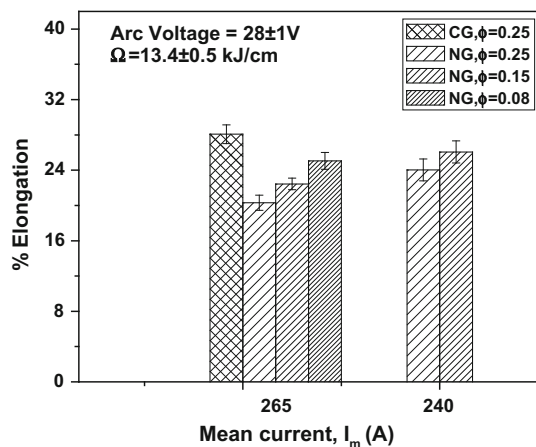


Fig. 25 Effect of I_m and ϕ on % elongation of MPMSPL-CG and MPSSPL-ENG P-GMA weld joints prepared at a given Ω of 13.4 ± 0.5 kJ/cm

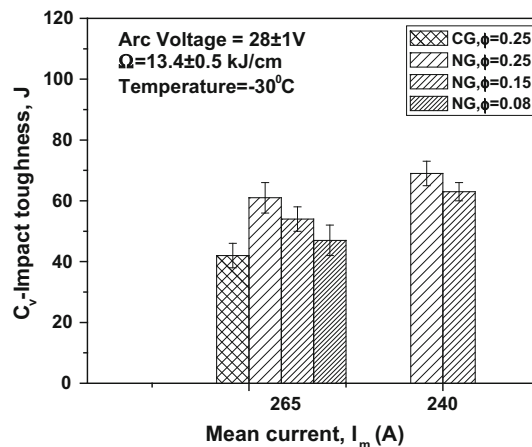


Fig. 27 Effect of I_m and ϕ on C_v impact toughness at -30°C of MPMSPL-CG and MPSSPL-ENG P-GMA weld joints prepared at a given Ω of 13.4 ± 0.5 kJ/cm

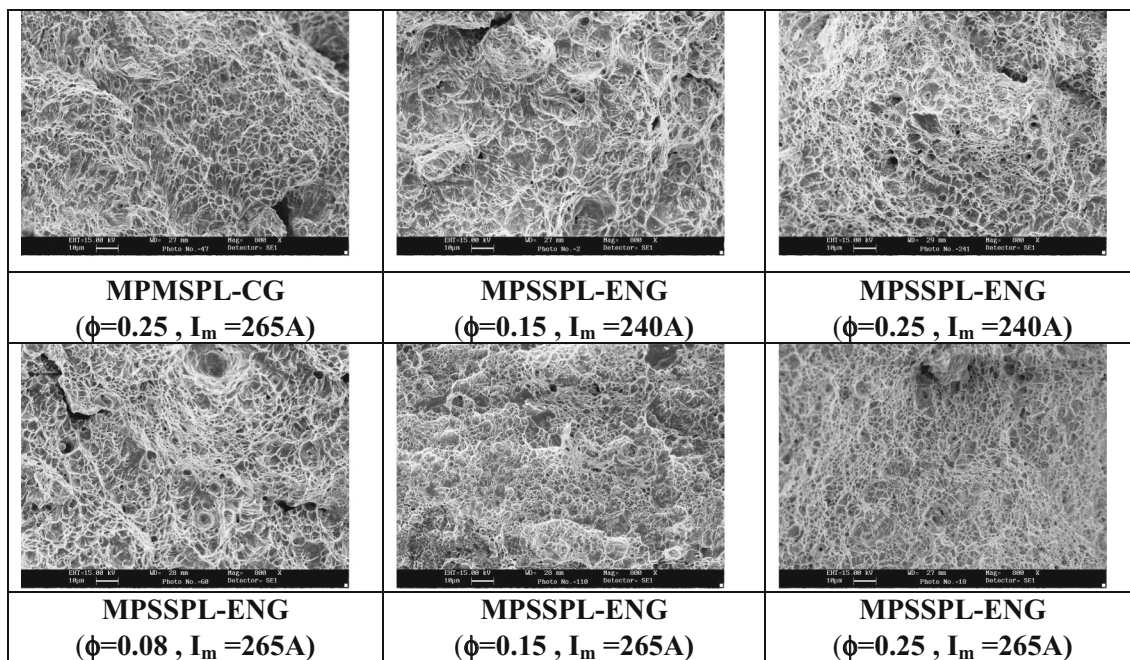


Fig. 26 Typical fractographs of all weld tensile specimens from the top of MPMSPL-CG and MPSSPL-ENG P-GMA weld prepared at a given Ω of 13.4 ± 0.5 kJ/cm at varied I_m and ϕ

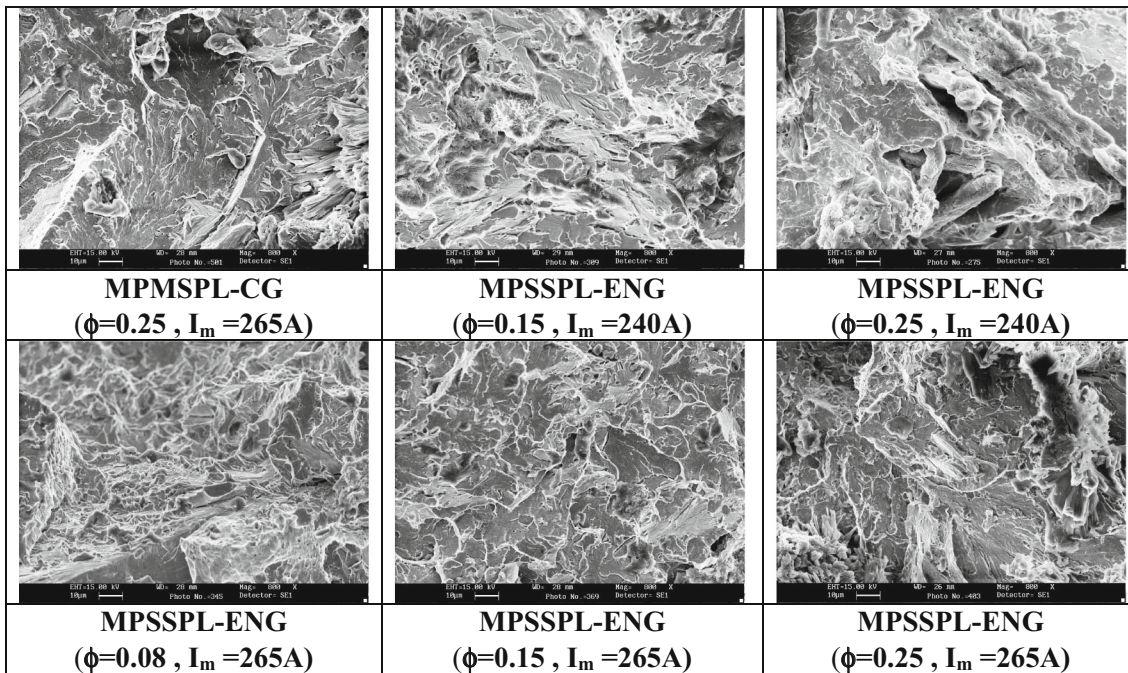


Fig. 28 Typical fractographs of C_V impact toughness specimen of MPMSPL-CG and MPSSPL-ENG P-GMA weld prepared at a given Ω of 13.4 ± 0.5 kJ/cm at different I_m and ϕ

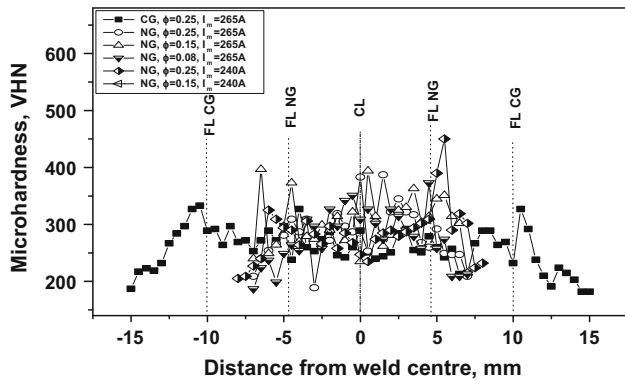


Fig. 29 Typical variation in hardness observed across the MPMSPL-CG and MPSSPL-ENG P-GMA weld joints prepared at a given Ω of 13.4 ± 0.5 kJ/cm at different I_m and ϕ

A relatively higher level of I_m and ϕ at lower Ω results into better mechanical and metallurgical properties of the weld joint. The improvement in properties of the MPSSPL-ENG weld has been found to be predominantly governed by the fraction of dendrite and its morphology as a function of pulse parameters affecting the thermal behavior of weld deposition.

References

- S.S. Babu and S.A. David, Inclusion Formation and Microstructure Evolution in Low Alloy Steel Weld, *ISIJ Int.*, 2002, **42**, p 1344–1353
- D.L. Olson, T.A. Siewert, S. Liu, and G.R. Edwards, *ASM Handbook-Welding, Brazing and Soldering*, Vol 6, ASM International, Materials Park, 1993, p 1–2873
- D. Radaj, *Heat Effects of Welding*, 1st ed., Springer, Berlin, 1992, p 1–348
- B.P. Agrawal and P.K. Ghosh, Thermal Modeling of Multi Pass Narrow Gap Pulse Current GMA Welding by Single Seam per Layer Deposition Techniques, *Mat. Manuf. Proc.*, 2010, **25**(11), p 1251–1268
- P.K. Ghosh, S.G. Kulkarni, B.P. Agrawal, High Deposition Pulse Current GMAW can Change Current Scenario of Thick Wall Pipe Welding, *Proceeding of International Conference on Pressure Vessel and Piping, ASME-2009, 26th–30th July*, Prague, Czech Republic, 2009, p 1755–1760
- V.K. Goyal, P.K. Ghosh, and J.S. Saini, Analytical Studies on Thermal Behavior and Geometry of Weld Pool in Pulsed Current Gas Metal Arc Welding, *J. Met. Proc. Technol.*, 2008, **209**, p 1318–1336
- V.K. Goyal, P.K. Ghosh, and J.S. Saini, Influence of Pulse Parameters on Characteristics of Bead on Plate Weld Deposits of Aluminium and Its Alloy in the Pulsed Gas Metal Arc Welding Processes, *Metall. Mater. Trans. A*, 2008, **39A**, p 3260–3275
- R. Kumar, R. Anant, P.K. Ghosh, A. Kumar, and B.P. Agrawal, Influence of PC-GTAW Parameters on the Microstructural and Mechanical Properties of Thin AISI 1008 Steel Joints, *J. Mater. Eng. Perform.*, 2016, **25**(9), p 3756–3765
- K. Devkumaran and P.K. Ghosh, Thermal Characteristics of Weld and HAZ during Pulse Current Gas Metal Arc Weld Bead Deposition on HSLA Steel Plate, *Mater. Manuf. Process.*, 2010, **25**(7), p 616–630
- P.K. Ghosh, L. Dorn, K. Devkumaran, and F. Hofmann, Pulsed Current Gas Metal Arc Welding under Different Shielding and Pulse Parameters Part-1: Arc Characteristics, *ISIJ Int.*, 2009, **49**(2), p 251–260
- P.K. Ghosh, L. Dorn, K. Devkumaran, and F. Hofmann, Pulsed Current Gas Metal Arc Welding under Different Shielding and Pulse Parameters Part-2: Behaviour of Metal Transfer, *ISIJ Int.*, 2009, **49**(2), p 261–269
- F.L. Singer and A. Pytel, *Strength of Materials*, 4th ed., Harper Collins Publisher, New York, 2009, p 1–469
- V.K. Goyal, P.K. Ghosh, and J.S. Saini, Process-Controlled Microstructure and Cast Morphology of Dendrite in Pulsed-Current Gas-Metal Arc Weld Deposits of Aluminium and Al-Mg Alloy, *Metall. Mater. Trans. A*, 2007, **38**(8), p 1794–1805
- P.K. Ghosh, L. Dorn, M. Hubner, and V.K. Goyal, Arc Characteristics and Behaviour of Metal Transfer in Pulsed Current GMA Welding of Aluminium Alloy, *J. Mater. Process. Technol.*, 2007, **194**, p 163–175
- P.K. Ghosh, L. Dorn, S. Kulkarni, and F. Hoffmann, Arc Characteristics and Behaviour of Metal Transfer in Pulsed Current GMA Welding of Stainless Steel, *J. Mater. Process. Technol.*, 2008, **209**, p 1262–1274

16. K. Devkumaran, Pulsed Current Narrow Gap Gas Metal Arc Welding of Thick HSLA Steel Plate, Thesis, Indian Institute of Technology, Roorkee, India, 2009
17. P.K. Ghosh, V.K. Goyal, H.K. Dhiman, and M. Kumar, Thermal and Metal Transfer Behaviours in Pulsed Current GMA Weld Deposition of Al-Mg Alloy, *Sci. Technol. Weld. Join.*, 2006, **11**(2), p 232–242
18. K.S. Gurunath, Narrow Gap Pulse Current Gas Metal Arc Welding of Thick Wall 304LN Stainless Steel Pipe, Thesis, Indian Institute of Technology, Roorkee, India, 2008
19. P.K. Ghosh, S.G. Kulkarni, M. Kumar, and H.K. Dhiman, Pulsed Current GMAW for Superior Weld Quality of Austenitic Stainless Steel Sheet, *ISIJ Int.*, 2007, **47**(1), p 138–145
20. S.S. Babu, The Mechanism of Acicular Ferrite in Weld Deposits, *Curr. Opin. Solid State Mater. Sci.*, 2004, **8**, p 267–278
21. S. Liu and D.L. Olson, The Role of Inclusions in Controlling HSLA Steel Weld Metal Microstructure, *Weld. J.*, 1986, **65**(6), p 139s–149s
22. B.P. Agrawal and P.K. Ghosh, Influence of Thermal Characteristics on Microstructure of Pulse Current GMA Weld Bead of HSLA Steel, *Int. J. Adv. Manuf. Technol.*, 2015, **77**, p 1681–1701
23. L.L. Wang, F.G. Lu, H.C. Cui, and X.H. Tang, Investigation on Thermal Inertia of GMAW-P Welding on Al Alloy, *Sci. Technol. Weld. Join.*, 2014, **20**(2), p 106–114